



Article

High-Performance Geopolymers with Municipal Solid Waste Incineration Fly Ash: Influence on the Mechanical and Environmental Properties

Xiaochen Lin ^{1,†} , Dapeng Zhang ^{1,†}, Zehua Zhao ¹, Cheng Zhang ¹, Bing Ma ¹, Hao Zhou ¹ , Yi Wang ^{1,*}, Dingming Xue ¹, Jing Tang ^{1,*}, Chen Chen ², Jing Li ³, Zengqing Sun ^{4,*}, Houhu Zhang ^{1,*} and Weixin Li ^{1,*}

¹ Nanjing Institute of Environmental Sciences (NIES), Ministry of Ecology and Environment of the People's Republic of China, Nanjing 210042, China

² College of Information Science and Technology & Artificial Intelligence, Nanjing Forestry University, Nanjing 210037, China; chenchen@njfu.edu.cn

³ Nanjing Research Institute of Environmental Protection, Nanjing 210013, China

⁴ School of Minerals Processing and Bioengineering, Central South University, Changsha 410083, China

* Correspondence: wangyi_nies@163.com (Y.W.); tangjing@nies.org (J.T.); sunzengqing@csu.edu.cn (Z.S.); zhanghouhu@nies.org (H.Z.); liweixin@nies.org (W.L.)

† These authors contributed equally to this work.

Abstract: Geopolymer is a sustainable low-carbon cementitious material that is able to incorporate large amounts of solid waste as precursors or activators. As the proportion of municipal solid waste incineration continues to rise in China, the large-scale generation of municipal solid waste incineration fly ash (MSWI FA) has emerged as a significant challenge. The production of geopolymers represents a potential pathway for the comprehensive utilization of MSWI FA. However, most studies have reported that geopolymers containing MSWI FA exhibit low strength, which diminishes their economic value. Furthermore, the unclear environmental risks associated with MSWI FA-based geopolymers have impeded their broader application. This study explores the use of MSWI FA as a substitute for ground granulated blast furnace slag (GGBS) or coal fly ash (CFA) in the production of high-performance geopolymers, achieving compressive strengths exceeding 60 MPa, even when the MSWI FA content reaches 50%. A synergistic effect is observed between MSWI FA and CFA, which enhances the reactivity of CFA. With reasonable formulation, the environmental risks of geopolymers containing MSWI FA are manageable in normal rainfall scenarios. However, there remains a potential risk of soil and groundwater contamination under extreme conditions, such as acid rain.

Keywords: geopolymer; MSWI FA; leaching



Citation: Lin, X.; Zhang, D.; Zhao, Z.; Zhang, C.; Ma, B.; Zhou, H.; Wang, Y.; Xue, D.; Tang, J.; Chen, C.; et al.

High-Performance Geopolymers with Municipal Solid Waste Incineration Fly Ash: Influence on the Mechanical and Environmental Properties.

Buildings **2024**, *14*, 3518. <https://doi.org/10.3390/buildings14113518>

Academic Editor: Bjorn Birgisson

Received: 12 October 2024

Revised: 27 October 2024

Accepted: 30 October 2024

Published: 4 November 2024



Copyright: © 2024 by the authors. Licensee MDPI, Basel, Switzerland. This article is an open access article distributed under the terms and conditions of the Creative Commons Attribution (CC BY) license (<https://creativecommons.org/licenses/by/4.0/>).

1. Introduction

The consumption of building materials is substantial. Annual global production of concrete exceeds 10 billion tons [1], being the most widely utilized material globally, surpassed only by water [2]. Traditional concrete employs Portland cement as a binder. The production of Portland cement clinker necessitates high-temperature calcination, requiring more than 3000 MJ of energy to produce a single ton [3]. Due to fuel consumption and the decomposition of calcium carbonate at high temperatures, approximately 0.8 tons of carbon dioxide emissions are produced out of one ton of cement on average [1,3,4]. Cement production accounts for 80% of the total carbon emissions in the building materials sector [5]. In the past half-century, the rapid development of infrastructure has led to a dramatic increase in cement production, of which annual output surpasses 4 billion tons [5–8]. China exhibits an enormous demand for building materials, with its cement production in recent years exceeding more than half of the global total [5]. The carbon emissions resulting from cement production contribute approximately 15% of China's total emissions, placing significant strain on the environment [9]. According to China's carbon

peaking and carbon neutrality strategy, the building materials sector is expected to achieve peak carbon emissions by 2030, highlighting an urgent need to lower the carbon emissions per unit volume of building materials.

Reducing the usage of Portland cement and developing low-carbon cementitious materials are crucial strategies for achieving carbon emissions peaking. Geopolymers, which do not contain cement and do not require high-temperature calcination, can achieve carbon emissions as low as 10% of ordinary Portland cement [10,11]. This makes geopolymer a novel and sustainable low-carbon cementitious material. Geopolymers were initially invented by Davidovits [12] and produced by using activators to activate the reactivity of silicoaluminates precursors, resulting in the polymerization of these precursors into a cement-like cementitious material. The activators typically are highly concentrated alkaline solutions, such as MOH, M_2CO_3 , or $M_2O \cdot (n)SiO_2$, where “M” represents an alkali metal element, usually sodium (Na^+) or potassium (K^+). During the polymerization, silicate tetrahedra $[SiO_4]^{4-}$ and aluminate tetrahedra $[AlO_4]^{5-}$ form a three-dimensional network structure, which accounts for the strength of geopolymers. The general formula for the reaction products is $M_n[-(SiO_2)_z-AlO_2]_n \cdot H_2O$, where “z” denotes the silicon-to-aluminum ratio and “n” indicates the degree of polymerization [13,14]. In recent years, multiple technical committees related to geopolymers have been established under the International Union of Laboratories and Experts in Construction Materials, Systems, and Structures (RILEM), and they have frequently presented keynote discussions at international conferences on cement chemistry [15–17]. Unlike conventional cementitious materials, which form a linear structure of C-S-H through hydration reactions, geopolymers undergo a polymerization process that produces an amorphous three-dimensional network, predominantly consisting of N-A-S-H or C-A-S-H gels [18]. As a result, geopolymers exhibit excellent mechanical properties, outstanding corrosion resistance, and low carbon emissions while allowing for substantial incorporation of industrial waste, making it a green alternative to traditional cement [17,19]. Particularly, the ability to incorporate large amounts of solid waste as precursors or activators makes geopolymers a potential solution for waste utilization. In well-formulated waste-based geopolymers, solid waste can provide aluminosilicates or alkali that enhance the mechanical properties of the geopolymers with economic benefits [20,21]. At the same time, the dense structure of geopolymers helps to minimize the leaching of heavy metals from solid waste, reducing the risk of environmental pollution and conserving landfill space [22,23]. This synergy between environmental management and building material research offers potential for both enhanced waste utilization and sustainable building materials.

In terms of environmental management, human activities inevitably generate municipal waste, which has negative effects on both human health and the environment [24]. The management of municipal solid waste is one of the greatest challenges faced by both developing and developed countries [25]. The United States, China, and India are the top three countries in terms of municipal solid waste generation worldwide [26]. According to data from the National Bureau of Statistics of China, the generation of municipal solid waste in China has rapidly increased alongside urbanization, rising from 171 million tons in 2012 to 244 million tons in 2022, while the rate of harmless disposal of municipal solid waste has also improved from 84.8% to 99.9% [27].

Technologies for municipal solid waste disposal include landfilling [28], incineration [29,30], anaerobic digestion [31], composting [32], and pyrolysis [33], among which landfilling and incineration are the most widely utilized technologies [24]. Prior to 2018, landfilling was the primary technology of municipal solid waste disposal in China. Due to the low waste-to-energy conversion efficiency and significant environmental risks associated with landfilling, the utilization efficiency in China was much lower than that in developed countries, such as Germany, Japan, and Singapore, where incineration predominates [34]. Since 2019, the quantity of municipal solid waste incineration in China surpassed that of landfill disposal. By 2022, the incineration rate approached 80%, particularly in the

economically advanced eastern region, where more than 85% of municipal solid waste is disposed of through incineration [27].

So far, incineration has become the predominant technology for municipal solid waste disposal in China. During the incineration process, municipal solid waste is burned to generate substantial thermal energy for electricity production. Effectively recovering chemical energy while decomposing the organic components of municipal solid waste, the incineration of municipal waste results in an 85–90% reduction in volume and a 65–80% reduction in mass [35,36]. However, incineration generates secondary wastes, including approximately 25–30% bottom ash and 3–5% fly ash, based on the weight of the incinerated waste [37,38]. The municipal solid waste incineration bottom ash, characterized by a low content of pollutants, is widely utilized as aggregates or supplementary cementitious materials in the manufacturing of building materials [39–41]. In contrast, the municipal solid waste incineration fly ash (MSWI FA) contains significant amounts of harmful substances, including salts, heavy metals (e.g., Zn, Pb, As, Hg, and Cd), and organic pollutants (e.g., dioxins, furans, and polycyclic aromatic hydrocarbons), and is classified as hazardous waste in many countries [42–44]. Based on the fact that the MSWI FA output is about 4% of the mass of municipal solid waste incinerated, the yield of MSWI FA in China was nearly 8 million tons in 2022, accounting for approximately 8% of the total hazardous waste generated that year [45]. The data indicate that the production of MSWI FA is substantial, and its disposal through landfilling consumes vast amounts of land. In densely populated cities in eastern China, it has become increasingly difficult to find suitable land for constructing landfills, presenting significant challenges for the disposal of MSWI FA. As various provinces and cities in China advance their “zero waste city” initiatives, China will continue to promote waste reduction and resource recovery, minimizing landfill disposal. Research and application of technologies for the utilization and harmless disposal of MSWI FA need to be strengthened.

Research on utilizing MSWI FA as a precursor for geopolymers is relatively limited. Chemically, the high content of silicoaluminate oxides in fluidized bed fly ash makes it more suitable for alkali activation than that from grate furnaces [46]. However, the predominant incineration technology in China is grate furnaces, which yield fly ash with insufficient silicoaluminate content to form a dense silicoaluminate three-dimensional network. The utilization of this MSWI FA with alkali activation alone poses challenges in achieving strength; therefore, it is necessary to incorporate other silicoaluminate precursors to create binary or even multicomponent geopolymers [47]. The strength of MSWI FA mixed with electrolytic manganese slag after alkali activation can reach 5 MPa [48]. When MSWI FA is mixed with coal fly ash, lime, and gypsum and subjected to steam curing, it can meet the mechanical requirements of 9.75 MPa for masonry blocks [49]. The use of coal fly ash in conjunction with MSWI FA for alkali activation can yield a cementitious material with a strength of 34 MPa after 28 days [50]. Achieving high mechanical strength in geopolymers using MSWI FA as a precursor is challenging, often necessitating the incorporation of high-value materials such as silica fume or nanomaterials to enhance the mechanical properties.

Numerous studies have investigated the use of geopolymers for the solidification/stabilization of MSWI FA [44,51,52]. It is generally believed that harmful substances in the MSWI FA are solidified/stabilized through physical and chemical mechanisms: on the one hand, the three-dimensional silicoaluminate network framework physically encapsulates harmful substances; on the other hand, the reaction products (C-A-S-H and N-A-S-H gels) possess negative charges, allowing harmful substances to be adsorbed onto the surfaces of the alkali-activated gels and their pore structures through chemical and electrostatic interactions [46].

This study utilizes MSWI FA in combination with ground granulated blast furnace slag (GGBS) and coal fly ash (CFA) as precursors to produce geopolymers through alkali activation. The research investigates how different precursor combinations of MSWI FA influence the mechanical and environmental properties of geopolymers while also

investigating the feasibility of producing a high-performance geopolymer with a substantial incorporation of MSWI FA (up to 50%).

2. Materials and Methods

2.1. Materials

2.1.1. Preparation of MSWI FA

The presence of a substantial amount of chlorides in MSWI FA can lead to the corrosion of reinforcing steel when used as a building material. This study utilizes MSWI FA that has been subjected to a washing process to remove chlorides. To select a representative sample of MSWI FA, six untreated, non-solidified chelated samples were collected from six municipal waste incineration plants across four cities in Jiangsu Province. Jiangsu is a typical economically developed province in eastern China, where the rate of municipal waste incineration reached 88.57% in 2022 [27]. The bulk chemical compositions of the untreated MSWI FA were analyzed by X-ray fluorescence (XRF) on a Thermo Scientific ARL 9900 X-ray WorkStation, as detailed in Table 1.

Table 1. Bulk chemical composition of untreated MSWI FA from Jiangsu Province, given in % by weight.

	Origin					
	City A-1	City A-2	City A-3	City B	City C	City D
Cl	26.08	27.58	50.01	25.24	15.47	20.54
Na ₂ O *	15.30	13.76	36.42	12.64	9.23	7.41
K ₂ O *	8.51	8.05	2.53	6.15	5.54	5.00
CaO	36.08	35.46	6.23	43.58	29.34	53.62
SO ₃	6.53	7.30	3.43	7.80	9.53	6.55
SiO ₂	2.38	6.26	2.94	6.69	8.16	5.61
Al ₂ O ₃	0.64	1.52	0.05	0.68	4.21	0.87
Fe ₂ O ₃	0.63	1.03	0.43	0.64	4.90	0.82
MgO	0.95	1.08	0.51	0.80	2.57	1.02
TiO ₂	0.24	0.68	0.02	0.29	1.19	0.22
P ₂ O ₅	0.44	0.53	0.19	0.40	1.01	0.33
ZnO	0.49	0.71	2.09	0.47	0.69	0.56
PbO	0.09	0.08	0.03	0.12	0.19	0.21
CuO	0.05	0.05	0.21	0.05	0.18	0.08

* Presented as oxides, yet they are more likely to exist as chlorides in MSWI FA.

Table 1 illustrates that the Cl content in MSWI FA from Jiangsu Province is notably high, ranging from 15.47 wt% to 50.01 wt%. The Cl in MSWI FA primarily originates from the thermal decomposition or volatilization of organic chlorine compounds and inorganic chlorides, which enter the flue gas in the form of HCl or metal chlorides. In air pollution control systems, HCl or metal chlorides from the flue gas condense into particulate matter or are captured by alkaline substances, remaining in the MSWI FA [53]. In recent years, China's implementation of waste classification policies has resulted in a higher Cl content in municipal solid waste, subsequently increasing the Cl content in MSWI FA [54]. The contents of Na and K are positively correlated with Cl content. According to the literature, chlorine in MSWI FA primarily exists in the form of chloride salts of sodium, potassium, and calcium [55,56]. Ca is the element with the highest content, aside from chlorine, whose content ranges from 6.23 wt% to 53.62 wt% when expressed as CaO. The contents of other components are generally low in untreated MSWI FA. The contents of SO₃ and SiO₂ are below 10 wt%, with some samples exceeding 5 wt%. The concentrations of Al₂O₃, Fe₂O₃, MgO, TiO₂, and P₂O₅ are below 5 wt%, with certain samples surpassing 1 wt%. Additionally, contaminants such as Zn, Pb, and Cu are present in the majority of samples at concentrations below 1 wt%. The above results indicate significant variations in the chemical composition of MSWI FA produced by different cities in Jiangsu Province and even within different regions of the same city. In subsequent experiments, MSWI FA from

City A-1, whose elemental composition is close to the average values, was selected as the material for further processing.

MSWI FA from City A-1 underwent a desalination treatment through water washing. Specifically, the MSWI FA was mixed with tap water at a weight ratio of 1:10 and continuously stirred to ensure adequate solid–liquid contact. After 120 min of washing, the mixture was subjected to vacuum filtration. Following four cycles of washing and filtering, the MSWI FA filter cake was placed in an oven and dried at 105 °C until reaching a constant weight, serving as the raw material for geopolymer preparation in this study. After washing, the Cl content in the MSWI FA decreased from 26.08 wt% to 0.842 wt%.

2.1.2. Precursors

In addition to MSWI FA, commercially available ground granulated blast furnace slag (GGBS) and coal fly ash (CFA) were also utilized in this study as precursors for geopolymer production. GGBS was sourced from a steel smelting enterprise in Jiangsu Province and meets the S105 grade as specified in the GB/T 18046-2017 standard [57], with a slag activity index of $\geq 105\%$. The CFA is obtained from a coal-fired power plant in Henan Province, China, and complies with the Class I standard of GB/T 1596-2017 [58], having a strength activity index of $\geq 70\%$. The chemical compositions of MSWI FA, GGBS, and CFA are presented in Table 2. After desalination, the MSWI FA exhibited a significant reduction in the contents of Na and K, while the concentrations of other components correspondingly increased. Among the three precursors, MSWI FA is predominantly composed of CaO, which exists in the forms of sulfates, carbonates, and hydroxides. It is the predominant component in GGBS, accompanied by SiO₂ and Al₂O₃. The chemical composition of CFA is primarily characterized by SiO₂ and Al₂O₃, with lower concentrations of the other components.

Table 2. Bulk chemical composition of the precursors, given in % by weight.

	MSWI FA	GGBS	CFA
CaO	48.14	40.86	6.46
SiO ₂	4.35	29.52	50.74
Al ₂ O ₃	1.41	15.68	23.07
SO ₃	7.98	2.47	1.38
MgO	2.31	8.53	0.63
Fe ₂ O ₃	1.19	0.29	9.03
TiO ₂	0.57	1.29	2.22
K ₂ O	0.26	0.32	2.55
Na ₂ O	0.32	0.44	0.17
P ₂ O ₅	0.92	0.02	1.04
MnO	0.06	0.37	0.72
BaO	0.07	0.05	0.62
SrO	0.03	0.07	0.17
ZrO ₂	0.01	0.04	0.14
Cl	0.84	0.04	ND

Powder XRD measurement was applied to explore the mineral composition of the precursors. The details about the measurement are given in Section 2.3.2. The XRD patterns are shown in Figure 1. The dominant perspective suggests that the reactivity in geopolymerization originates from the amorphous phases of the precursors [59,60]. In the XRD patterns of GGBS, no strong diffraction peaks but rather a broad peak between 20 and 40° 2 θ are observed, indicating that GGBS is predominantly composed of amorphous phases. Superimposed on this broad peak are three smaller diffraction peaks corresponding to minor amounts of akermanite, calcite, and merwinite. CFA shows a broad peak around 15–35° 2 θ , indicating the presence of a significant amount of amorphous phases. Additionally, CFA contains crystalline phases, primarily composed of quartz, mullite, and hematite.

In contrast, MSWI FA exhibits more defined crystallinity with no apparent broad peak, and its main crystalline phases include calcite, gypsum, syngenite, and quartz.

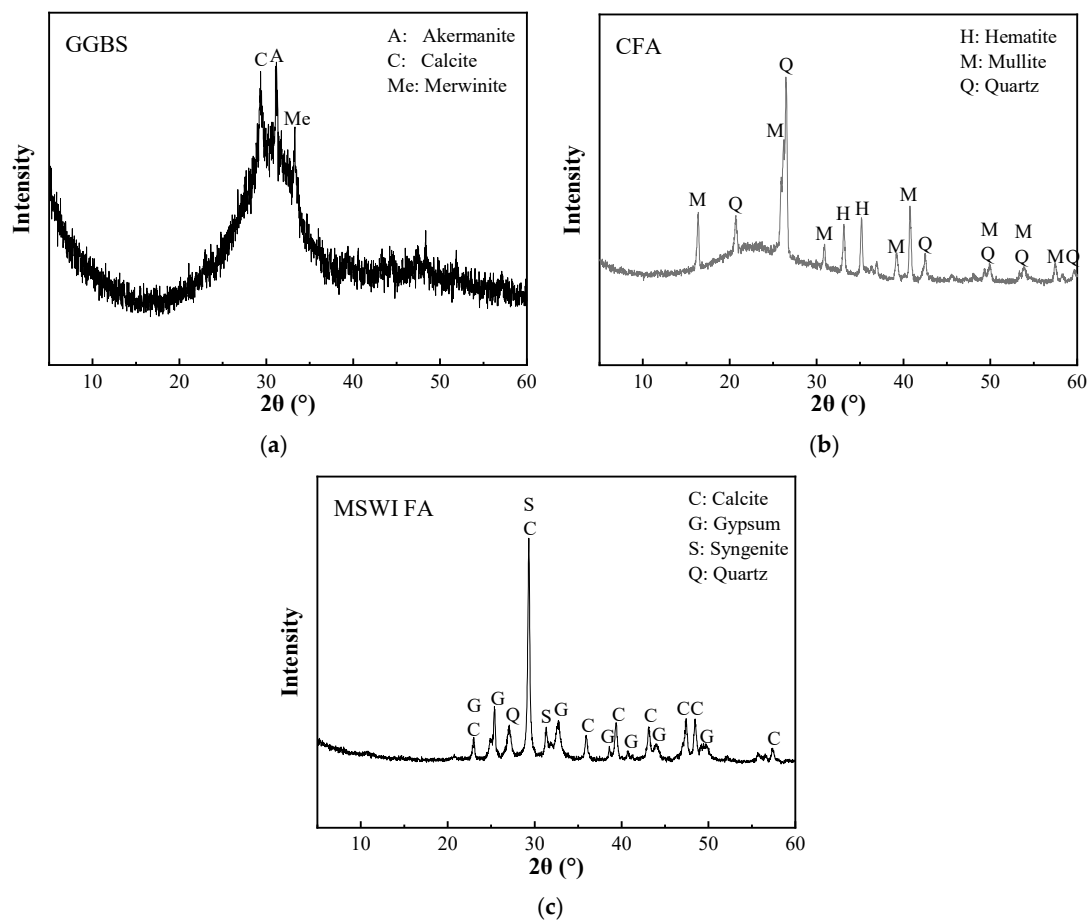


Figure 1. XRD pattern of precursors: (a) GGBS, (b) CFA, and (c) MSWI FA.

2.2. Mix Proportions and Preparation

A series of experiments were performed based on geopolymer matrixes of GGBS, CFA, and combinations of GGBS and CFA. MSWI FA, which was desalinated using the method described in Section 2.1.1, was used to partially replace GGBS or CFA. The replacement levels of fly ash were set at 25% or 50%, resulting in a total of eight formulations. Table 3 provides the mixed proportions of the geopolymers produced in this study. To demonstrate the reactivity of the precursor mix proportions, each mixture employed an equal amount of NaOH and sodium silicate as the activator, with an activator-to-precursor ratio, denoted as liquid-solid ratio (L/S), of 0.7.

Table 3. Mix proportions of geopolymers, given in % by weight.

Sample Number	GGBS	CFA	MSWI FA	Activator	Notes
G100	100	0	0	70	GGBS Matrix
G75M25	75	0	25	70	
G50M50	25	0	50	70	
C100	0	100	0	70	CFA Matrix
C75M25	0	75	25	70	
C50M50	0	25	50	70	
G50C50	50	50	0	70	Mixed Matrix
G50C25M25	50	25	25	70	

First, the pre-weighed precursor materials were premixed at low speed for 60 s to ensure the materials were thoroughly and uniformly mixed. The activator was then added to the mixer, followed by mixing at low speed for 60 s. After a 15 s pause, the mixing resumed at high speed for another 60 s. The resulting geopolymer paste was cast into molds and compacted on a vibrating table. Cube specimens with a side length of 40 mm were used, with each sample cast in two layers, vibrating continuously until air was completely expelled from the paste. Once the pastes were too sticky, a plastic stick was used to compact the pastes manually.

2.3. Characterization

2.3.1. Compressive Strength

The cast geopolymer samples were sealed with a film along with their molds to prevent surface drying and loss of moisture and were cured at 20 °C for 24 h. After 24 h, the molds were removed, and the samples were labeled and sealed with a film to isolate them from the air, continuing to cure at 20 °C and 95% relative humidity until testing to prevent moisture loss or carbonation.

Each mixture of geopolymers was tested for compressive strength at 3, 7, 14, and 28 days, using three samples as replicates for each test. The compressive strength of the geopolymers was evaluated according to GB/T 17671-2021 [61], where the samples were placed in a hydraulic press and subjected to a continuous loading rate of 2400 ± 200 N/s until failure. The maximum pressure the material could withstand, divided by the loading area, yielded the compressive strength of the material. This method also complies with the European standard EN 196-1:2016 [62].

2.3.2. Mineralogical Measurement

The mineralogical compositions of both precursors and geopolymers were analyzed using X-ray diffraction (XRD). Geopolymer samples were made according to the mix design and cured under the same conditions as the previous samples for compressive strength. After 14 d curing, the geopolymers were crushed to pass 1 mm sieve. Approximately 3 g crushed particles were mixed with 100 mL isopropanol for 15 min to stop the reactions. The mixture was then filtered and rinsed using isopropanol and diethyl ether, followed by a drying process in a vacuum oven at 40 °C and manually ground using agate mortar to pass through a 63 μm sieve. The samples were stored in a desiccator to prevent carbonation prior to XRD measurement.

The mineral phases of geopolymer samples were determined with Rigaku D/max-2200PC. Cu K α X-ray was generated under operating conditions of 40 kV and 30 mA, with data collected over a 2θ range of 5~90° in theta–theta geometry. The scan step size was set at 0.02° 2θ , with a scanning speed of 2° 2θ /min. XRD measurements of the source precursors were conducted using the same configuration. The obtained diffraction patterns were analyzed using HighScore Plus software version 5.1.

2.3.3. Functional Group Analysis

The functional groups and chemical bonds of precursors and geopolymers were analyzed using Fourier-transform infrared spectroscopy (FTIR). Geopolymer samples were cured under the same conditions as the XRD samples after mixing. After 14 days of curing, the geopolymers were crushed and ground using a vibrating mill to pass through a 63 μm sieve. Then, the samples were dried at 105 °C for 2 h. The samples were analyzed promptly after preparation.

The FTIR samples were analyzed using a Thermo Scientific Nicolet iS20 spectrometer after being pressed into pellets with KBr. The scanning range was set from 400 to 4000 cm^{-1} , with a resolution of 4 cm^{-1} .

2.3.4. Leaching Test for Normal Rainfall

Geopolymer samples were cured under the same conditions as the samples for compressive strength. After 14 d curing, the geopolymers were carefully split. From the fragments of each geopolymer, 2–3 pieces with a diameter of approximately 1–2 cm were selected and weighed. These were placed into PE bottles, and distilled water was added at a liquid-to-solid ratio of 10:1. The bottle caps were tightly sealed, and the bottles were placed on a rotary shaker, rotating at a speed of 30 revolutions per minute for 24 h. Solid–liquid separation was then conducted through filtration, and the eluate was collected for analysis.

The pH of the eluate was immediately measured using a pH electrode after the leaching process was completed. The concentrations of Cd, Cr, Cu, Mn, Ni, Pb, and Zn were determined using a Thermo Scientific iCAP RQ Inductively Coupled Plasma Mass Spectrometer (ICP-MS). The concentrations of As and Hg in the eluate were analyzed using an AFS-933 atomic fluorescence spectrometer (Titan Instruments, Beijing, China). The concentration of Cr (VI) was measured according to the method specified in GB/T 15555.4-1995 [63], involving a reaction with 1,5-Diphenylcarbohydrazide and spectrophotometric measurement at the maximum absorption wavelength of 540 nm.

2.3.5. Leaching Test for Acid Rain

The sample preservation, pre-treatment, and testing methods for leaching tests for acid rain are consistent with those for leaching tests for normal rainfall, differing only in the eluent used. In leaching tests for acid rain, a water solution acidified with sulfuric acid and nitric acid is employed as the eluent to simulate acid rain. Specifically, a mixture of concentrated sulfuric acid and concentrated nitric acid in a mass ratio of 2:1 is added to distilled water, adjusting the pH to 3.20 ± 0.05 .

3. Results and Discussions

3.1. Mechanical Properties of Geopolymers

Strength is the most critical characteristic of structural building materials. High-strength building materials enable the production of structural components with reduced cross-sectional areas, which not only saves materials but also significantly reduces the self-weight of the materials—an aspect of great importance for bridges and skyscrapers. Therefore, the application of high-strength building materials holds substantial value. However, in most studies focused on producing building materials with MSWI FA, the mechanical strength is typically low, limiting their value and hindering the comprehensive utilization of MSWI FA.

According to the strength and durability requirements of modern building structures, normal-strength concrete (NSC) with a compressive strength of 30 MPa can meet the strength demands of most architectural frameworks. Concrete with a compressive strength exceeding 60 MPa after 28 days is classified as high-strength concrete (HSC) or high-performance concrete (HPC), while concrete with a compressive strength exceeding 100 MPa is termed ultra-high strength concrete or ultra-high performance concrete (UHPC) [64]. With its exceptional strength and broad application potential in bridges and skyscrapers, UHPC has become a research hotspot in the field of concrete over the past two decades, representing a high-value building material.

This study investigates the reactivity of MSWI FA in different matrices, exploring the potential of using MSWI FA to produce HPC or UHPC, thereby achieving its high-value application.

3.1.1. GGBS Matrix

The compressive strength of geopolymers based on the GGBS matrix is shown in Figure 2. The geopolymer using 100% GGBS precursor achieved a compressive strength exceeding 100 MPa within just 3 days, meeting the performance requirements for UHPC and surpassing 140 MPa in 28 days. Based on this formulation, MSWI FA was used to replace 25% or 50% of the GGBS precursor. Although the compressive strength of the

formulation with 25% MSWI FA replacement was lower than that of the pure GGBS sample, the early compressive strength developed rapidly, reaching over 60 MPa in 3 days, meeting the requirements for HPC. By 7 days, the compressive strength had reached approximately 90 MPa, after which it grew more slowly, achieving 95 MPa in 28 days, close to the performance threshold for UHPC. For the formulation with 50% MSWI FA replacement, the compressive strength exceeded 60 MPa after 7 days, meeting the HPC requirements, and reached 72 MPa in 28 days, lower than both the pure GGBS formulation and the 25% MSWI FA replacement formulation.

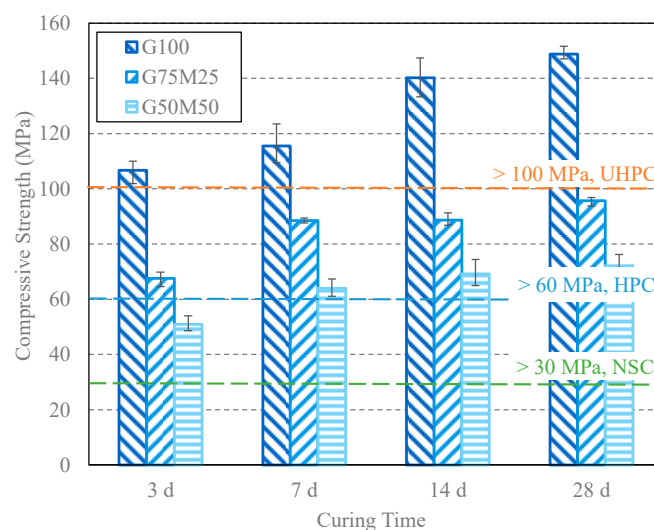


Figure 2. Compressive strength of geopolymers based on GGBS matrix.

From the FTIR analysis, it can be observed that the 100% GGBS geopolymer exhibits no significant changes compared to the original GGBS precursor, aside from slight differences in peak intensities (see Figure 3). The peak near 480 cm^{-1} corresponds to the bending vibration of the Si-O bond, while the absorption peak near 980 cm^{-1} represents the stretching vibration of the Si-O bond. The intensity of the Si-O bond-related signals decreases with the addition of desalinated MSWI FA, corresponding to a reduction in SiO_2 content in the precursor mixture. The absorption peak near 1435 cm^{-1} is associated with the symmetric stretching vibration of CO_3^{2-} , which increases as the amount of MSWI FA increases, indicating a higher carbonate content in the system due to the MSWI FA addition. The absorption peak near 1635 cm^{-1} corresponds to the stretching vibration of C=C bonds, while the broad absorption peak around 3450 cm^{-1} is due to the stretching vibration of O-H bonds. After the incorporation of MSWI FA into the GGBS, a new absorption peak appears near 870 cm^{-1} , corresponding to the bending vibration of C-H bonds in the benzene rings of dioxins and other aromatic organic pollutants in the MSWI FA. The signal of this 870 cm^{-1} peak becomes more pronounced as the MSWI FA content increases.

The XRD analysis reveals that the diffraction peaks of the geopolymers with 100% GGBS show no significant changes compared with the GGBS precursor, with a broad hump appearing around $30^\circ 2\theta$, indicating that the mineral phases are predominantly in an amorphous state (see Figure 4). However, after the addition of MSWI FA, a sharp peak appears at $29.3^\circ 2\theta$, corresponding to the diffraction peak of calcite crystals introduced by the washed MSWI FA. The intensity of this calcite peak increases with the rising proportion of MSWI FA.

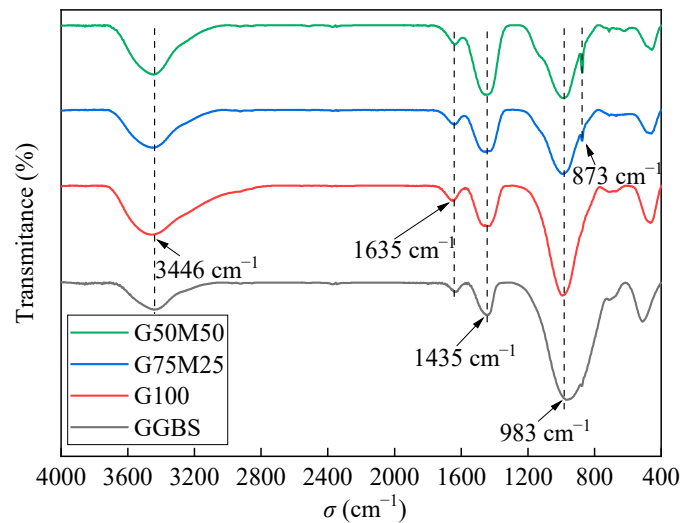


Figure 3. FTIR analysis of geopolymers based on GGBS matrix.

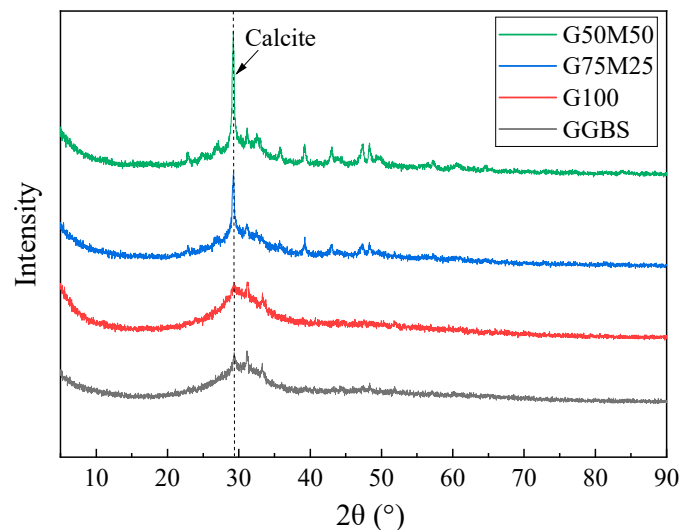


Figure 4. XRD analysis of geopolymers based on GGBS matrix.

3.1.2. CFA Matrix

The pure CFA precursor formulation (C100) was unable to develop any strength. Based on the CFA matrix, MSWI FA was used to replace 25% or 50% of the CFA precursor to react with an activator. The formulation with 25% MSWI FA replacement resulted in a certain level of strength after the reaction. However, the overall compressive strength remained low, with a 28-day compressive strength of 28.3 MPa (see Figure 5), which did not meet the 30 MPa strength standard for structural materials. Nevertheless, this could be applied in ordinary structures with lower strength requirements, such as beams, slabs, columns, stairs, and trusses. As the MSWI FA content increased, the compressive strength of the CFA-based geopolymer with 50% MSWI FA replacement further improved, exceeding 60 MPa in 7 days, reaching the performance level of HPC. The strength reached 71.5 MPa in 14 days, which is comparable to the geopolymer with 50% MSWI FA replacement in the GGBS precursor (G50M50, see Figure 2). While the reactivity and strength of the CFA precursor are significantly lower than those of the GGBS precursor, the combined use of CFA and MSWI FA precursors synergistically activated the reactivity of both, resulting in a high-strength geopolymer comparable to that produced with the GGBS precursor.

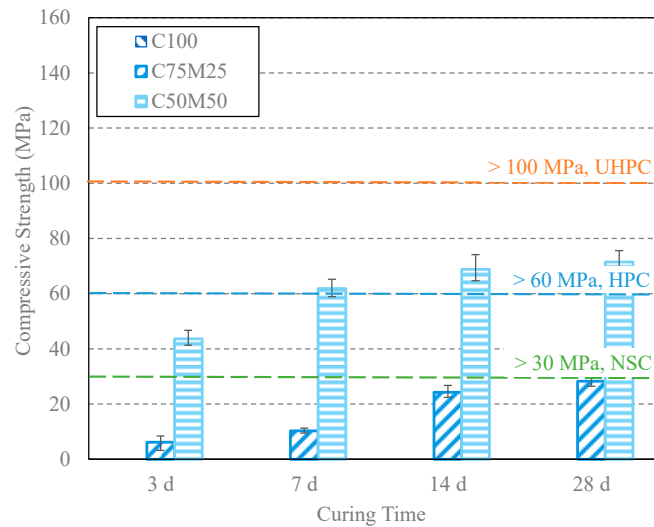


Figure 5. Compressive strength of geopolymers based on CFA matrix.

The FTIR analysis results of CFA-based geopolymers are shown in Figure 6. The CFA precursor shows a characteristic absorption peak around 1100 cm^{-1} for SO_4^{2-} , indicating the presence of sulfates in the CFA. A stretching vibration absorption peak for C=C bonds is observed near 1640 cm^{-1} , and a broad absorption peak for O-H bond stretching vibrations appears around 3450 cm^{-1} . These peaks are largely retained after the incorporation of MSWI FA in the synergistic reaction. In the composite binder of CFA and MSWI FA, the characteristic SO_4^{2-} peak around 1100 cm^{-1} shifts toward 1020 cm^{-1} , likely due to the formation of ettringite or monosulfate mineral phases. Additionally, in the CFA-based geopolymers with MSWI FA, a new absorption peak emerges around 1450 cm^{-1} , corresponding to the symmetric stretching vibration of CO_3^{2-} , and another appears near 870 cm^{-1} , attributed to the bending vibration of C-H bonds in the benzene rings of dioxins and other aromatic organic pollutants. The intensity of the peaks at 1450 cm^{-1} and 870 cm^{-1} increases with the amount of MSWI FA, indicating that MSWI FA introduces carbonates and benzene ring-containing organic pollutants such as dioxins into the system.

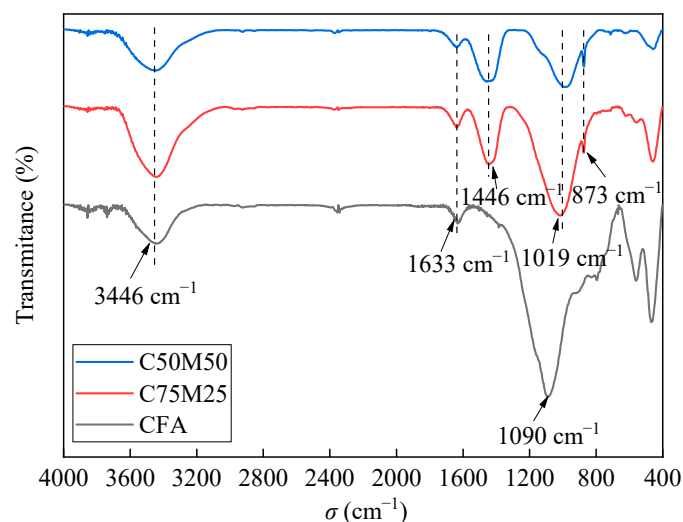


Figure 6. FTIR analysis of geopolymers based on CFA matrix.

In comparison to the CFA precursor, the CFA-based geopolymer with 25% MSWI FA shows no significant changes in crystal composition, except for the appearance of a calcite (CaCO_3) diffraction peak at $29.3^\circ 2\theta$ (see Figure 7). Additionally, the broad hump initially present around $22^\circ 2\theta$ shifts to $25^\circ 2\theta$, indicating that some amorphous phases in

the CFA have reacted with MSWI FA, forming N-A-S-H and C-A-S-H gel phases. In the CFA-based geopolymer with 50% MSWI FA, the calcite diffraction peak at $29.3^\circ 2\theta$ becomes more pronounced with increased MSWI FA content, while the mullite and quartz peaks disappear. The broad hump around $22^\circ 2\theta$ further shifts to $30^\circ 2\theta$, suggesting that the degree of reaction has significantly increased compared to the 25% MSWI FA replacement formulation, as quartz and mullite react with MSWI FA to form N-A-S-H and C-A-S-H gels. Combined with the compressive strength results of the geopolymer (see Figure 7), it is evident that the addition of MSWI FA enhances the reactivity of CFA.

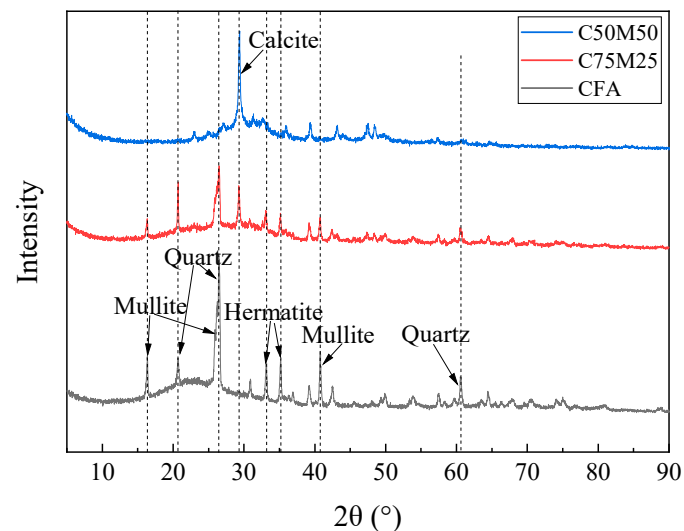


Figure 7. XRD analysis of geopolymers based on CFA matrix.

3.1.3. Mixed Matrix

In addition to the formulations where CFA and GGBS were used individually as primary precursors, this study also designed a composite geopolymer with equal proportions of GGBS and CFA, each accounting for 50% of the precursor mixture. This material exhibited a compressive strength exceeding 60 MPa in 7 days and over 100 MPa in 28 days, which is approximately 70% of the strength of the pure GGBS-based geopolymer, meeting the performance criteria for UHPC (see Figure 8).

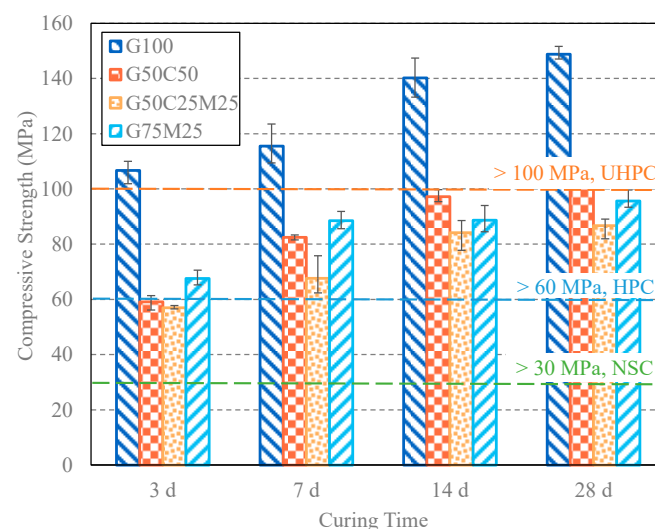


Figure 8. Compressive strength of geopolymers based on mixed matrix of GGBS and CFA.

Based on this composite GGBS-CFA geopolymer, a ternary precursor formulation was designed by replacing 25% of the CFA with MSWI FA, resulting in GGBS, CFA, and MSWI

FA contents of 50%, 25%, and 25%, respectively. The compressive strength of this material showed little change in 3 days, and while the 7-day strength was slightly lower than the formulation without MSWI FA, it still exceeded 60 MPa, meeting HPC performance requirements. By 28 days, the compressive strength reached about 80% of the formulation without MSWI FA.

Derived from this ternary geopolymer, further replacing the remaining 25% CFA with a more reactive GGBS resulted in a GGBS-MSFA precursor mix of 75% GGBS and 25% MSWI FA. Although this formulation exhibited higher early strength compared to the ternary mix, the 28-day strength did not show significant improvement. This suggests a synergistic effect between MSWI FA and the CFA precursor, indicating that a well-balanced combination of MSWI FA and CFA can effectively replace the highly reactive GGBS precursor.

By comparing the FTIR spectra of the GGBS-CFA composite formulation with equal amounts of each precursor (G50C50), the ternary formulation (G50C25M25), and the GGBS-MSWI FA composite formulation (G75M25), it can be observed that the FTIR spectra are largely consistent across all three formulations. Variations in the proportions of GGBS or CFA in the precursors do not result in significant differences in the FTIR spectra (as shown in Figure 9). However, the formulations containing MSWI FA exhibit an absorption peak of around 870 cm^{-1} , corresponding to the bending vibration of the C-H bond in aromatic rings, which is associated with dioxins and other organic pollutants present in the MSWI FA.

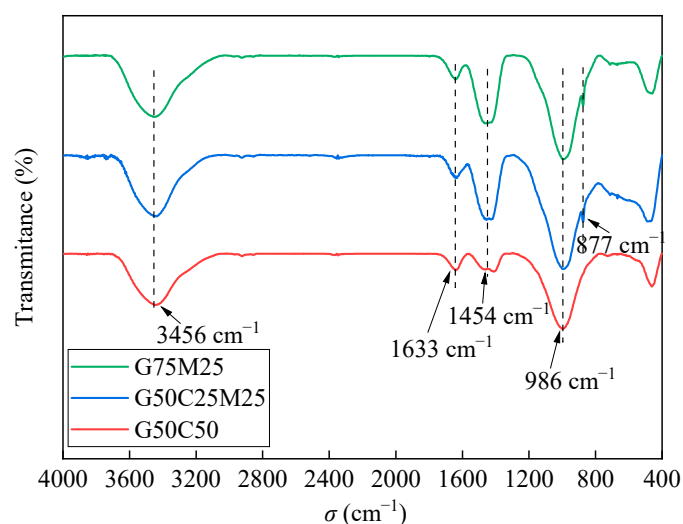


Figure 9. FTIR analysis of geopolymers based on mixed matrix of GGBS and CFA.

3.1.4. Comparison with Literature Data

In comparison with existing literature, this study demonstrates a notable improvement in compressive strength for geopolymers containing substantial MSWI FA content. Previous studies commonly report that geopolymers incorporating MSWI FA generally exhibit low compressive strengths, especially when MSWI FA content exceeds 20 wt%, due to its limited reactivity (see Table 4). For instance, efforts to enhance strength through high-temperature treatment [50] or by adding costly nanomaterials [65] have yielded improvements but have often failed to meet the HPC threshold of 60 MPa.

In this study, however, the incorporation of 25–50% MSWI FA into GGBS and CFA-based geopolymer matrices resulted in 28 d compressive strengths ranging from 71.5 to 95.6 MPa, meeting and exceeding the HPC requirements. This outcome highlights that through the rational design of raw material combinations, MSWI FA can indeed be utilized effectively in the development of high-value building materials. This finding contrasts with the lower strength values reported in most previous studies and suggests that tailored composition strategies can unlock MSWI FA's potential in high-performance applications.

Table 4. Comparison of compressive strength of geopolymers with MSWI FA.

Reference	Precursors	Activator	L/S	Curing	Compressive Strength, MPa	Notes
[44]	MSWI FA 70%, CFA 30%	NaOH	0.60	20 ± 2 °C, RH > 90%	22.4 (28 d)	Optimal CFA content of 30% was identified within a range of 10–50%
[47]	MSWI FA 90%, metakaolin 10%	NaOH and Na ₂ SiO ₃	0.65	20 ± 2 °C, RH > 90%	20.53 (90 d)	Metakaolin enhanced strength, though the impact of varying metakaolin content was not examined
[48]	MSWI FA 75%, electrolytic manganese residue (EMR) 25%	NaOH	0.50	25 °C, RH 90%	1.47 (28 d)	Compressive strength of geopolymers decreased as the EMR content increased (EMR content 20–35%)
[49]	MSWI FA 20.5%, CFA 41.7%, quicklime 14.2%, gypsum 23.6%	NaOH	0.16	220 °C 10 h autoclaved	8.39	NaCl and NaNO ₃ were used as substitutes for NaOH, resulting in autoclaved bricks with strengths ranging from 8 to 10 MPa
[50]	MSWI FA 20%, CFA 80%	NaOH and Na ₂ SiO ₃	0.48	Ambient temp. 24 h, then 100 °C 7 h	34.3	Both strength and setting time decreased as the MSWI FA content in the precursor increased
[52]	MSWI FA 5%, metakaolin 95%	NaOH and Na ₂ SiO ₃	0.69	20 °C, RH 90%, covered with polyethylene films	Approx. 32.5 (28 d)	When MSWI FA content ≤ 5%, the 28 d compressive strength remained nearly constant, while the 7 d and 14 d strengths increased. However, the 28 d strength decreased significantly when the MSWI FA content > 5%
[65]	MSWI FA 10%, CFA 88.5%, nano SiO ₂ 1.5%	NaOH and Na ₂ SiO ₃	0.56	Ambient temp. in sealed plastic bags	Approx. 57 (28 d)	Nanomaterials contribute to enhancing the compressive strength of geopolymers
	MSWI FA 10%, CFA 88%, nano-γ-Al ₂ O ₃ 2%				Approx. 57 (28 d)	
This work	MSWI FA 25%, GGBS 75%	NaOH and Na ₂ SiO ₃	0.7	20 °C sealed with plastic film	95.6	High-performance MSWI FA geopolymers were successfully developed, achieving 28-day compressive strength exceeding 60 MPa
	MSWI FA 25%, GGBS 50%, CFA 25%				86.7	
	MSWI FA 50%, GGBS 50%				72.1	
	MSWI FA 50%, CFA 50%				71.5	

3.1.5. Contribution to Strength

The reactivity of MSWI FA and CFA is significantly lower than that of GGBS; therefore, the role of MSWI FA and CFA in the material cannot be simply assessed based on the absolute strength values. In this case, the blended strength index (BSI) is used to evaluate the contribution of MSWI FA and CFA to the strength.

$$BSI = f_{t,FA} / (f_{t,GGBS} \cdot \omega_{GGBS}) \quad (1)$$

where $f_{t,FA}$ represents the compressive strength of geopolymers containing MSWI FA or CFA at age t ; $f_{t,GGBS}$ denotes the strength of pure GGBS-based geopolymer at the same age t ; and ω_{GGBS} refers to the proportion of GGBS in the mixture.

In the BSI, GGBS geopolymer is considered the matrix. If MSWI FA and CFA are non-reactive and work merely as filler, with the strength entirely provided by the matrix, the strength would be proportional to the GGBS content, resulting in $BSI = 1$. If $BSI > 1$, it indicates that MSWI FA or CFA have participated in the reaction, contributing positively to the strength. Conversely, if $BSI < 1$, it suggests that the incorporation of MSWI FA and CFA has a negative impact on the material's strength.

The BSI calculation results for geopolymers containing MSWI FA and CFA at different ages are presented in Figure 10. In the geopolymers with MSWI FA and GGBS as a binary mixed precursor, the BSI for MSWI FA ranges between 0.85 and 1.1, approaching 1, indicating that MSWI FA primarily serves as filler in this binary system, contributing little to strength development. For the geopolymers with CFA and GGBS as a binary mixed precursor, the BSI is approximately 1.1 at 3 days and maintains around 1.4 after 7 days, suggesting that CFA effectively promotes strength development, albeit at a slower reaction rate, significantly contributing to later strength. A similar phenomenon is observed in the alkali-activated materials with MSWI FA, CFA, and GGBS as a ternary precursor system, where the BSI is greater than 1, primarily contributing to later strength but remaining lower than that of the CFA and GGBS binary formulation. This indicates that the synergistic effect between GGBS and CFA is stronger than that between MSWI FA and CFA. In the existing literature, the substantial addition of MSWI FA often significantly reduces the strength of geopolymers [50,52]. In contrast, this study shows that with high MSWI FA content (25% or 50%), the BSI generally remains around 1 or even exceeds 1, indicating that within this formulation system, MSWI FA either contributes positively to strength or, at the very least, remains inert without adversely affecting strength.

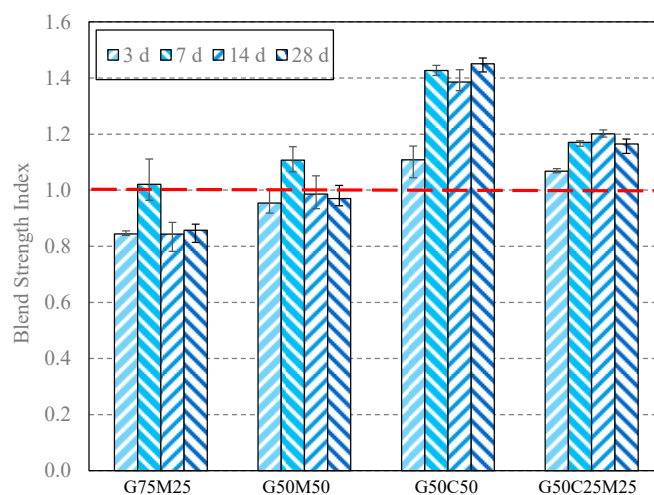


Figure 10. Blend strength index of geopolymers with MSWI FA and CFA.

3.2. Environmental Properties of Geopolymers

Under the current technological conditions, washing can effectively remove chloride from MSWI FA, while thermal treatment can decompose organic pollutants such as dioxins.

However, there are no economically viable methods for extracting heavy metals that remain in the treated MSWI FA. This retention may pose negative environmental impacts when MSWI FA is utilized in building materials. The environmental risks associated with geopolymers containing MSWI FA require thorough evaluation.

This study focuses on geopolymers that serve as substitutes for cement in building materials. Typically, they are not designed for direct human contact but are commonly used in applications such as exterior walls, foundations, and tunnel support structures, exposing them to environmental conditions. The heavy metals contained in these materials may leach into the environment due to rainfall or groundwater immersion, leading to potential contamination of surrounding soil and groundwater, thereby impacting human health.

The environmental risk assessment in this study is conducted at two levels. The first level evaluates the leaching of geopolymers under normal rainfall conditions, comparing the concentration of heavy metals in the eluate to China's comprehensive wastewater discharge standards (GB 8978-1996 [66]). If the concentration of a geopolymer's eluate falls below the standard limit, it is deemed that the environmental risk of that geopolymer is manageable, allowing for its use in scenarios that are distant from human contact. The second level assesses the leaching of geopolymers under acid rain conditions, again comparing the eluate's heavy metal concentration to China's groundwater concentration limits. If the eluate concentration of a geopolymer is below the groundwater concentration limit in a specific area, it indicates that the geopolymer can be widely utilized in that region, even under adverse environmental conditions, without concerns about potential environmental pollution.

3.2.1. For Normal Rainfall

Geopolymers were leached using distilled water to simulate normal rainfall, following the method described in Section 2.3.4. The eluate was evaluated for As, Cd, Cr, Cr(VI), Cu, Hg, Mn, Ni, Pb, and Zn based on China's comprehensive wastewater discharge standard (GB 8978-1996 [66]).

Cd and Mn were not detected in the eluate of any geopolymers.

Pb, Cr, Cu, and Zn were only detected in the eluate of a small number of geopolymers, with the highest eluate concentrations originating from the geopolymer using pure CFA as the precursor yet still remaining far below the wastewater limit (see Figure 11).

As, Hg, Ni, and Cr(VI) were detected in nearly all geopolymers, with the concentrations of Hg, Ni, and Cr(VI) in all geopolymers, as well as As concentrations in most geopolymers, being significantly below the wastewater limits.

Notably, in the precursor formulation of 75% CFA combined with 25% MSWI FA (C75M25), the As concentration reached 712 $\mu\text{g/L}$, exceeding the wastewater limit of 500 $\mu\text{g/L}$. In contrast, the eluate from the pure CFA precursor geopolymer showed no detectable As concentration; similarly, the eluate from the 50% CFA combined with 50% MSWI FA precursor formulation (C50M50) had an As concentration of only 10.8 $\mu\text{g/L}$. This indicates that the increased As leaching concentration cannot be solely attributed to the precursor materials but rather results from an inappropriate formulation. The MSWI FA enhanced the reactivity of CFA, promoting a more rapid dissolution of CFA and MSWI FA under alkaline activation, thus releasing previously fixed As from the solid phase into the solution. However, at lower MSWI FA content, the compressive strength of the material remains low, suggesting that the reaction to form new crystalline phases proceeds slowly, preventing the re-solidification of dissolved As and resulting in anomalously high As concentrations under specific formulation.

Overall, with the exception of the arsenic concentration in the specific formulation (C75M25), the concentrations of heavy metals in the eluate of all geopolymers, including those containing MSWI FA, were below the wastewater discharge standards. This indicates that, as long as the formulation is appropriate, the environmental risks posed by MSWI FA in geopolymers are manageable.

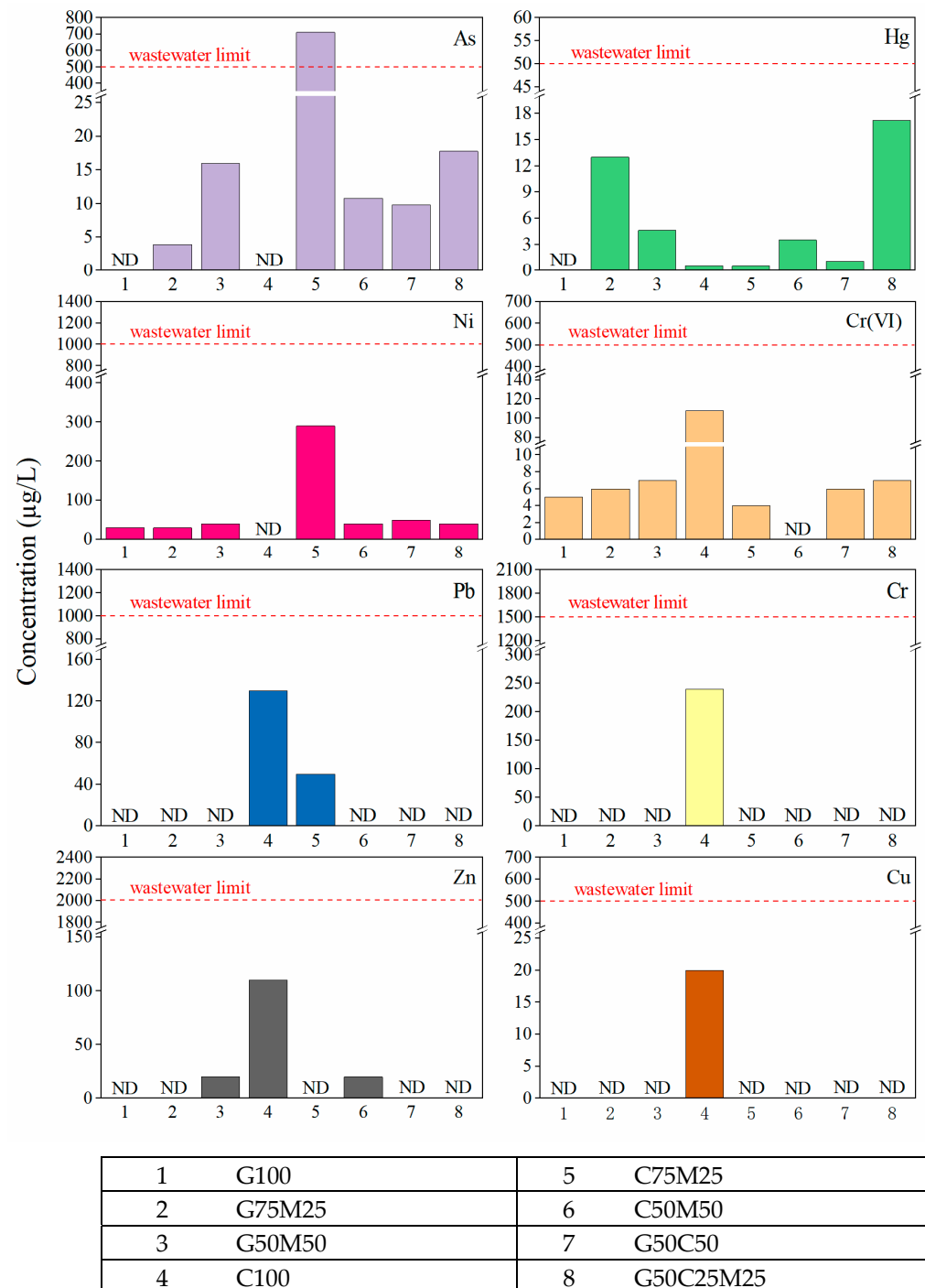


Figure 11. Concentration of eluate from the leaching tests for normal rainfall compared to wastewater discharge limits.

3.2.2. For Acid Rain

Geopolymers were leached under simulated acid rain conditions using water acidified with sulfuric and nitric acids, following the method described in Section 2.3.5. The eluate was evaluated for As, Cd, Cr, Cr(VI), Cu, Hg, Mn, Ni, Pb, and Zn in accordance with the groundwater quality standard set by GB/T 14848-2017 [67].

Cd and Mn were similarly undetected in the eluate obtained from the acid leaching process, indicating their good stability within the geopolymer system.

Cu and Pb were only detected in the eluate from the 75% CFA and 25% MSWI FA formulation (C75M25), suggesting that this formulation, due to its unreasonable composition,

reacted slowly and exhibited weaker stabilization capabilities for Cu and Pb compared to the other geopolymers in this study. Notably, the Cu concentration was significantly below the Class III groundwater limit, while the Pb concentration exceeded the Class III limit but remained below the Class IV groundwater limit (see Figure 12).

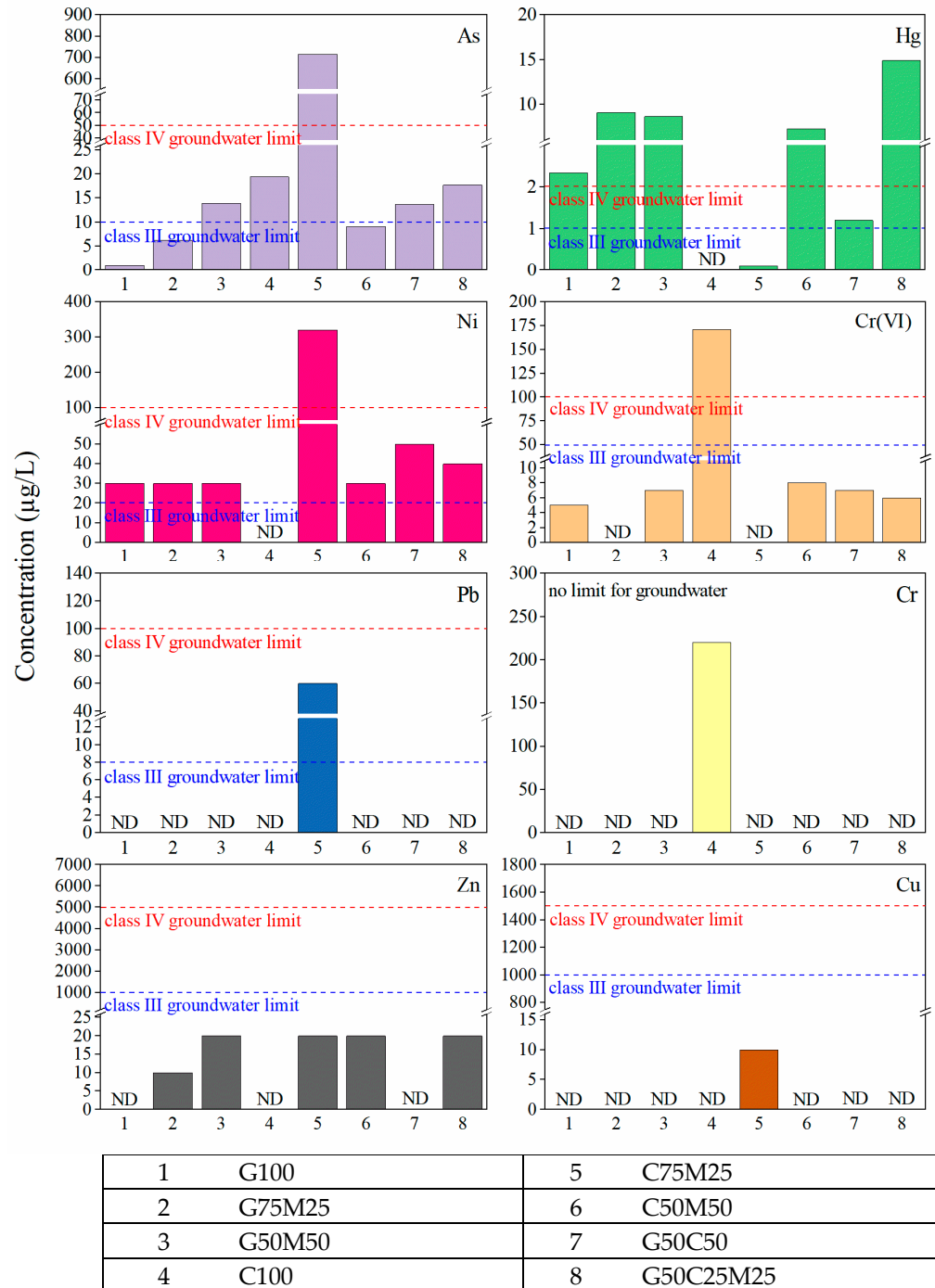


Figure 12. Concentration of eluate from the leaching tests for acid rain compared to groundwater quality standard.

Cr was only detected in the pure CFA precursor formulation; however, there are no limit requirements for Cr specified in GB/T 14848.

Zn was undetected in all formulations without MSWI FA (Nr. 1, 4, and 7), while it was present in all formulations containing MSWI FA (Nr. 2, 3, 5, 6, and 8). This indicates a potential correlation between the leaching of Zn and the presence of MSWI FA. How-

ever, all the leaching concentrations of Zn were significantly below the limits for Class III groundwater.

As, Hg, Ni, and Cr(VI) were detected in nearly all geopolymer formulations. In all formulations containing MSWI FA, the concentration of Cr(VI) was below the Class III groundwater limits. Only the geopolymer with the pure CFA precursor exhibited a Cr(VI) concentration that exceeded both Class III and Class IV groundwater limits, indicating that common general solid waste has the potential to contribute to groundwater pollution.

Except for the geopolymer with the pure CFA precursor, where nickel was not detected, all other geopolymers exhibited nickel concentrations that exceeded Class III groundwater limits; however, most remained below Class IV groundwater limits. Only the formulation comprising 75% CFA and 25% MSWI FA (C75M25) showed a nickel concentration that surpassed Class IV groundwater limits by a factor of 2.2.

The eluate from the pure CFA and the CFA-based formulation containing 25% MSWI FA met the Class III groundwater requirements for Hg concentration. The formulation comprising 50% GGBS and 50% CFA (G50C50) exhibited a Hg concentration exceeding the Class III groundwater limits but remaining below the Class IV limits. In contrast, all GGBS formulations (with MSWI FA content ranging from 0% to 50%), the formulation with 50% CFA and 50% MSWI FA (C50M50), as well as the formulation with 50% GGBS combined with 25% CFA and 25% MSWI FA (G50C25M25), showed Hg concentrations that surpassed Class IV groundwater limits.

The As concentrations in the 100% GGBS formulation (G100), the 75% GGBS and 25% MSWI FA formulation (G75M25), and the 50% CFA and 50% MSWI FA formulation (C50M50) meet the Class III groundwater requirements. In contrast, the As concentrations in the 50% GGBS and 50% MSWI FA formulation (G50M50), the pure CFA formulation (C100), the 50% GGBS and 50% CFA formulation (G50C50), and the formulation containing 50% GGBS with 25% CFA and 25% MSWI FA (G50C25M25) exceed Class III limits but remain below Class IV limits. The As concentration in the 75% CFA and 25% MSWI FA formulation (C75M25) surpasses the Class IV groundwater limits by 13.2 times, indicating a significant risk of contaminating groundwater.

The results indicate that the pure CFA precursor formulation (C100) and the 75% CFA combined with 25% MSWI FA formulation (C75M25) exhibit slow mechanical strength development due to their inappropriate composition, resulting in insufficient stabilization of heavy metals. This has led to elevated leaching concentrations of As, Cr(VI), Ni, and Pb, thereby posing a risk of groundwater contamination. In contrast, the leaching concentrations of the other geopolymer formulations remain below Class IV groundwater limits, except for Hg. The leaching of mercury from geopolymers appears to be a common phenomenon that requires further investigation.

4. Conclusions and Outlooks

4.1. Conclusions

This study involved the utilization of MSWI FA as a substitute for GGBS or CFA precursors in GGBS- and CFA-based geopolymers. The impact of MSWI FA on mechanical and environmental properties was evaluated, leading to the following conclusions:

High-performance geopolymers can be achieved with compressive strengths meeting HPC standards (≥ 60 MPa) even when the MSWI FA content is as high as 50% in both GGBS and CFA matrices. Geopolymers incorporating MSWI FA exhibit excellent early strength, with several formulations containing 25% to 50% MSWI FA achieving compressive strengths near or exceeding 60 MPa within 3 days, thereby meeting HPC strength requirements. Geopolymers prepared solely from MSWI FA and CFA do not develop strength independently; however, a synergistic effect exists between MSWI FA and CFA. In contrast, geopolymers derived from MSWI FA/CFA composite precursor formulations can meet HPC standards (≥ 60 MPa). The inclusion of MSWI FA facilitates the activation of low-reactivity CFA. The incorporation of MSWI FA has raised the Ca content in the

precursor mixture of CFA-based geopolymers, resulting in a more balanced elemental composition of the precursor mixture and facilitating the polymerization reaction.

For the leaching tests simulating normal rainfall, leaching concentrations of As, Cd, Cr, Cr(VI), Cu, Hg, Mn, Ni, Pb, and Zn in the eluate from the vast majority of geopolymers in this study, including all formulations with an MSWI FA precursor content of 50%, were below the Chinese wastewater discharge standards. An exception was noted for one poorly formulated precursor (C75M25), which exhibited As concentrations exceeding the standard limit. This indicates that, with reasonable formulations, the environmental risks associated with geopolymers containing MSWI FA are manageable. For the leaching tests simulating acid rain, the eluate concentrations of As, Hg, Ni, as well as Pb and Cr(VI) from several formulations of geopolymers, including those with and without MSWI FA, exceeded the Chinese Class III groundwater quality limits. This suggests that under extreme conditions such as acid rain, geopolymers may still pose a potential risk of contaminating soil and groundwater. Notably, certain MSWI FA/CFA combinations exhibited elevated As leaching concentrations, warranting further investigation in future studies. When considering the use of MSWI FA geopolymers in scenarios where extreme environmental conditions may occur, attention should be paid to formulating the material properly to minimize its inherent environmental risks. Additionally, protective construction techniques can be employed, such as embedding MSWI FA geopolymer structures beneath dense asphalt layers, thereby limiting their direct exposure to extreme conditions like acid rain.

4.2. Outlooks

This study represents an initial attempt to apply MSWI FA in high-value building materials, demonstrating that geopolymers containing substantial MSWI FA content (up to 50%) can achieve considerable mechanical strength while maintaining manageable environmental safety under normal rainfall conditions. However, many mechanisms remain to be elucidated, necessitating further research:

- (1) The reaction mechanisms between MSWI FA and precursors like GGBS and CFA. Advanced analyses such as thermogravimetric analysis (TGA), calorimetry, and XRD could be employed to study the evolution of crystalline phases during the reaction, providing a theoretical basis for optimizing raw material combinations.
- (2) The long-term environmental risks associated with MSWI FA-containing geopolymers. Building materials are frequently exposed to rainwater and atmospheric CO₂, leading to carbonation and a gradual decrease in pH. Further studies should investigate the aging-induced changes in heavy metal speciation within MSWI FA-based geopolymers, as well as their leaching behavior under varied degrees of carbonation, pH, and liquid-to-solid ratios. This would offer a comprehensive understanding of the lifecycle environmental safety of MSWI FA geopolymers.

Author Contributions: Conceptualization, X.L. and J.L.; methodology, Y.W.; validation, X.L., D.Z. and H.Z. (Hao Zhou); formal analysis, B.M. and D.X.; investigation, X.L., D.Z. and Z.Z.; resources, Z.S.; data curation, J.T. and C.Z.; writing—original draft preparation, X.L., C.C. and D.Z.; writing—review and editing, X.L. and D.Z.; supervision, H.Z. (Houhu Zhang) and W.L.; project administration, X.L. and J.T.; funding acquisition, Y.W. and Z.S. All authors have read and agreed to the published version of the manuscript.

Funding: This research was funded by National Key R&D Program of China (grant no. 2022YFC3901405), Central Public-interest Scientific Institution Basal Research Fund (grant no. GYZX230413, GYZX240201, GYZX240406 and GYZX200304), Postdoctoral Research Fund Program of Jiangsu Province (grant no. 2021K234B), Startup Funding for Faculty Research in Nanjing Forestry University (grant no. 163070183), and Nanjing Environmental Protection Research Fund (grant no. 202213).

Data Availability Statement: The data used in this study can be required from the corresponding author. The data are not publicly available due to information that could compromise research participant privacy.

Conflicts of Interest: The authors declare no conflict of interest.

References

1. Provis, J.L.; Bernal, S.A. Geopolymers and Related Alkali-Activated Materials. *Annu. Rev. Mater. Res.* **2014**, *44*, 299–327. [CrossRef]
2. Aitcin, P.-C. Cements of yesterday and today. *Cem. Concr. Res.* **2000**, *30*, 1349–1359. [CrossRef]
3. Schorcht, F.; Kourti, I.; Scalet, B.M.; Roudier, S.; Sancho, L.D. *Best Available Techniques (BAT) Reference Document for the Production of Cement, Lime and Magnesium Oxide: Industrial Emissions Directive 2010/75/EU (Integrated Pollution Prevention and Control)*; Publications Office: Luxembourg, 2013.
4. Gartner, E. Industrially interesting approaches to “low-CO₂” cements. *Cem. Concr. Res.* **2004**, *34*, 1489–1498. [CrossRef]
5. Bernhardt, D.; Reilly, J.F. (Eds.) *Mineral Commodity Summaries 2020*; U.S. Geological Survey: Reston, VA, USA, 2020.
6. van Oss, H.G.; Curry, K.C.; Hatfiel, A.K. Cement statistics, in comps. In *Historical statistics for mineral and material commodities in the United States: U.S. Geological Survey Data Series 140*; Kelly, T.D., Matos, G.R., Eds.; U.S. Geological Survey: Reston, VA, USA, 2020. Available online: <https://www.usgs.gov/centers/national-minerals-information-center/historical-statistics-mineral-and-material-commodities> (accessed on 29 October 2024).
7. Jewell, S.; Kimball, S.M. (Eds.) *Mineral Commodity Summaries 2017*; U.S. Geological Survey: Reston, VA, USA, 2017.
8. Zinke, R.K.; Werkheiser, W.H. (Eds.) *Mineral Commodity Summaries 2018*; U.S. Geological Survey: Reston, VA, USA, 2018.
9. Olivier, J.G.I.; Peters, J.A.H.W. *Trends in Global CO₂ and Total Greenhouse Gas Emissions 2019 Report*; PBL Netherlands Environmental Assessment Agency: Hague, The Netherlands, 2020.
10. Shi, C.; Roy, D.M.; Krivenko, P.V. *Alkali-Activated Cements and Concretes*; Taylor & Francis: Abingdon, UK, 2006.
11. Rasaki, S.A.; Bingxue, Z.; Guarecuco, R.; Thomas, T.; Yang, M. Geopolymer for use in heavy metals adsorption, and advanced oxidative processes: A critical review. *J. Clean. Prod.* **2019**, *213*, 42–58. [CrossRef]
12. Davidovits, J. Geopolymers: Inorganic Polymeric New Materials. *J. Therm. Anal.* **1991**, *37*, 1633–1656. [CrossRef]
13. Ren, B.; Zhao, Y.; Bai, H.; Kang, S.; Zhang, T.; Song, S. Eco-friendly geopolymer prepared from solid wastes: A critical review. *Chemosphere* **2020**, *267*, 128900. [CrossRef] [PubMed]
14. Ji, Z.; Pei, Y. Bibliographic and visualized analysis of geopolymer research and its application in heavy metal immobilization: A review. *J. Environ. Manag.* **2019**, *231*, 256–267. [CrossRef]
15. Shi, C.; Jimenez, A.F.; Palomo, A. New cements for the 21st century: The pursuit of an alternative to Portland cement. *Cem. Concr. Res.* **2011**, *41*, 750–763. [CrossRef]
16. Provis, J.L.; Palomo, A.; Shi, C. Advances in understanding alkali-activated materials. *Cem. Concr. Res.* **2015**, *78*, 110–125. [CrossRef]
17. Shi, C.; Qu, B.; Provis, J.L. Recent progress in low-carbon binders. *Cem. Concr. Res.* **2019**, *122*, 227–250. [CrossRef]
18. Bernal, S.A.; Provis, J.L. Durability of Alkali-Activated Materials: Progress and Perspectives. *J. Am. Ceram. Soc.* **2014**, *97*, 997–1008. [CrossRef]
19. Wu, Y.; Lu, B.; Bai, T.; Wang, H.; Du, F.; Zhang, Y.; Cai, L.; Jiang, C.; Wang, W. Geopolymer, green alkali activated cementitious material: Synthesis, applications and challenges. *Constr. Build. Mater.* **2019**, *224*, 930–949. [CrossRef]
20. Azad, N.M.; Samarakoon, S.S.M. Utilization of Industrial By-Products/Waste to Manufacture Geopolymer Cement/Concrete. *Sustainability* **2021**, *13*, 873. [CrossRef]
21. Tchakouté, H.K.; Rüscher, C.H.; Kong, S.; Kamseu, E.; Leonelli, C. Thermal Behavior of Metakaolin-Based Geopolymer Cements Using Sodium Waterglass from Rice Husk Ash and Waste Glass as Alternative Activators. *Waste Biomass Valorization* **2017**, *8*, 573–584. [CrossRef]
22. Zhang, Y.; Sun, W.; She, W.; Sun, G. Synthesis and heavy metal immobilization behaviors of fly ash based geopolymer. *J. Wuhan Univ. Technol. Sci. Ed.* **2009**, *24*, 819–825. [CrossRef]
23. Guo, B.; Pan, D.; Liu, B.; Volinsky, A.A.; Fincan, M.; Du, J.; Zhang, S. Immobilization mechanism of Pb in fly ash-based geopolymer. *Constr. Build. Mater.* **2017**, *134*, 123–130. [CrossRef]
24. Khan, S.; Anjum, R.; Raza, S.T.; Bazai, N.A.; Ihtisham, M. Technologies for municipal solid waste management: Current status, challenges, and future perspectives. *Chemosphere* **2022**, *288*, 132403. [CrossRef]
25. Kundariya, N.; Mohanty, S.S.; Varjani, S.; Ngo, H.H.; Wong, J.W.C.; Taherzadeh, M.J.; Chang, J.-S.; Ng, H.Y.; Kim, S.-H.; Bui, X.-T. A review on integrated approaches for municipal solid waste for environmental and economical relevance: Monitoring tools, technologies, and strategic innovations. *Bioresour. Technol.* **2021**, *342*, 125982. [CrossRef] [PubMed]
26. Nanda, S.; Berruti, F. Municipal solid waste management and landfilling technologies: A review. *Environ. Chem. Lett.* **2021**, *19*, 1433–1456. [CrossRef]
27. National Bureau of Statistics; Ministry of Ecology and Environment (Eds.) *China Statistical Yearbook on Environment 2023*; China Statistics Press: Beijing, China, 2023.
28. Laner, D.; Crest, M.; Scharff, H.; Morris, J.W.; Barlaz, M.A. A review of approaches for the long-term management of municipal solid waste landfills. *Waste Manag.* **2012**, *32*, 498–512. [CrossRef]
29. Evangelisti, S.; Tagliaferri, C.; Clift, R.; Lettieri, P.; Taylor, R.; Chapman, C. Life cycle assessment of conventional and two-stage advanced energy-from-waste technologies for municipal solid waste treatment. *J. Clean. Prod.* **2015**, *100*, 212–223. [CrossRef]
30. Soltani, A.; Sadiq, R.; Hewage, K. Selecting sustainable waste-to-energy technologies for municipal solid waste treatment: A game theory approach for group decision-making. *J. Clean. Prod.* **2016**, *113*, 388–399. [CrossRef]
31. Van Fan, Y.; Klemeš, J.J.; Lee, C.T.; Perry, S. Anaerobic digestion of municipal solid waste: Energy and carbon emission footprint. *J. Environ. Manag.* **2018**, *223*, 888–897. [CrossRef] [PubMed]

32. Diaz, L.F.; Golueke, C.G.; Savage, G.M.; Eggerth, L.L. *Composting and Recycling Municipal Solid Waste*, 1st ed.; CRC Press: Boca Raton, FL, USA, 2020.
33. Arena, U. Process and technological aspects of municipal solid waste gasification: A review. *Waste Manag.* **2012**, *32*, 625–639. [[CrossRef](#)] [[PubMed](#)]
34. Ding, Y.; Zhao, J.; Liu, J.-W.; Zhou, J.; Cheng, L.; Zhao, J.; Shao, Z.; Iris, Ç.; Pan, B.; Li, X.; et al. A review of China's municipal solid waste (MSW) and comparison with international regions: Management and technologies in treatment and resource utilization. *J. Clean. Prod.* **2021**, *293*, 126144. [[CrossRef](#)]
35. Hjelmar, O. Disposal strategies for municipal solid waste incineration residues. *J. Hazard. Mater.* **1996**, *47*, 345–368. [[CrossRef](#)]
36. Tillman, D.A.; Rossi, A.J.; Vick, K.M. *Incineration of Municipal and Hazardous Solid Wastes*; Academic Press: San Diego, CA, USA, 1989.
37. Quina, M.J.; Bontempi, E.; Bogush, A.; Schlumberger, S.; Weibel, G.; Braga, R.; Funari, V.; Hyks, J.; Rasmussen, E.; Lederer, J. Technologies for the management of MSW incineration ashes from gas cleaning: New perspectives on recovery of secondary raw materials and circular economy. *Sci. Total Environ.* **2018**, *635*, 526–542. [[CrossRef](#)]
38. Jiang, X.; Chang, W. Review for treatment and application of municipal solid waste incineration fly ash. *J. Zhejiang Univ. Technol.* **2015**, *43*, 7–17.
39. Chen, B.; Zuo, Y.; Zhang, S.; de Lima Junior, L.M.; Liang, X.; Chen, Y.; van Zijl, M.B.; Ye, G. Reactivity and leaching potential of municipal solid waste incineration (MSWI) bottom ash as supplementary cementitious material and precursor for alkali-activated materials. *Constr. Build. Mater.* **2023**, *409*, 133890. [[CrossRef](#)]
40. Chen, B.; Perumal, P.; Aghabeyk, F.; Adediran, A.; Illikainen, M.; Ye, G. Advances in using municipal solid waste incineration (MSWI) bottom ash as precursor for alkali-activated materials: A critical review. *Resour. Conserv. Recycl.* **2024**, *204*, 107516. [[CrossRef](#)]
41. Chen, B.; Ye, G. The role of water-treated municipal solid waste incineration (MSWI) bottom ash in microstructure formation and strength development of blended cement pastes. *Cem. Concr. Res.* **2024**, *178*, 107440. [[CrossRef](#)]
42. Huang, T.; Liu, L.; Zhou, L.; Yang, K. Operating optimization for the heavy metal removal from the municipal solid waste incineration fly ashes in the three-dimensional electrokinetics. *Chemosphere* **2018**, *204*, 294–302. [[CrossRef](#)] [[PubMed](#)]
43. Li, W.; Sun, Y.; Huang, Y.; Shimaoka, T.; Wang, H.; Wang, Y.-N.; Ma, L.; Zhang, D. Evaluation of chemical speciation and environmental risk levels of heavy metals during varied acid corrosion conditions for raw and solidified/stabilized MSWI fly ash. *Waste Manag.* **2019**, *87*, 407–416. [[CrossRef](#)] [[PubMed](#)]
44. Fan, C.; Wang, B.; Ai, H.; Qi, Y.; Liu, Z. A comparative study on solidification/stabilization characteristics of coal fly ash-based geopolymer and Portland cement on heavy metals in MSWI fly ash. *J. Clean. Prod.* **2021**, *319*, 1287900. [[CrossRef](#)]
45. Ministry of Ecology and Environment, Annual Report on Ecological and Environmental Statistics in China, 2022. 2023. Available online: <https://www.mee.gov.cn/hjzl/sthjzk/sthjtnb/202312/W020231229339540004481.pdf> (accessed on 29 October 2024).
46. Xu, P.; Zhao, Q.; Qiu, W.; Xue, Y.; Li, N. Microstructure and Strength of Alkali-Activated Bricks Containing Municipal Solid Waste Incineration (MSWI) Fly Ash Developed as Construction Materials. *Sustainability* **2019**, *11*, 1283. [[CrossRef](#)]
47. Liu, J.; Hu, L.; Tang, L.; Ren, J. Utilisation of municipal solid waste incinerator (MSWI) fly ash with metakaolin for preparation of alkali-activated cementitious material. *J. Hazard. Mater.* **2021**, *402*, 123451. [[CrossRef](#)]
48. Zhan, X.; Wang, L.; Hu, C.; Gong, J.; Xu, T.; Li, J.; Yang, L.; Bai, J.; Zhong, S. Co-disposal of MSWI fly ash and electrolytic manganese residue based on geopolymeric system. *Waste Manag.* **2018**, *82*, 62–70. [[CrossRef](#)]
49. Guo, X.; Zhang, T. Utilization of municipal solid waste incineration fly ash to produce autoclaved and modified wall blocks. *J. Clean. Prod.* **2020**, *252*, 119759. [[CrossRef](#)]
50. Diaz-Loya, E.I.; Allouche, E.N.; Eklund, S.; Joshi, A.R.; Kupwade-Patil, K. Toxicity mitigation and solidification of municipal solid waste incinerator fly ash using alkaline activated coal ash. *Waste Manag.* **2012**, *32*, 1521–1527. [[CrossRef](#)]
51. Zhou, X.; Zhang, T.; Wan, S.; Hu, B.; Tong, J.; Sun, H.; Chen, Y.; Zhang, J.; Hou, H. Immobilization of heavy metals in municipal solid waste incineration fly ash with red mud-coal gangue. *J. Mater. Cycles Waste Manag.* **2020**, *22*, 1953–1964. [[CrossRef](#)]
52. Tan, J.; Dan, H.; Li, J. Use of municipal waste incineration fly ashes (MSWI FA) in metakaolin-based geopolymer. *Environ. Sci. Pollut. Res.* **2022**, *29*, 80727–80738. [[CrossRef](#)]
53. Ma, W.; Wenga, T.; Frandsen, F.J.; Yan, B.; Chen, G. The fate of chlorine during MSW incineration: Vaporization, transformation, deposition, corrosion and remedies. *Prog. Energy Combust. Sci.* **2020**, *76*, 100789. [[CrossRef](#)]
54. Liu, Z.; Fang, W.; Cai, Z.; Zhang, J.; Yue, Y.; Qian, G. Garbage-classification policy changes characteristics of municipal-solid-waste fly ash in China. *Sci. Total Environ.* **2023**, *857*, 159299. [[CrossRef](#)] [[PubMed](#)]
55. Zhu, F.; Takaoka, M.; Shiota, K.; Oshita, K.; Kitajima, Y. Chloride chemical form in various types of fly ash. *Environ. Sci. Technol.* **2008**, *42*, 3932–3937. [[CrossRef](#)]
56. Liu, Z.; Yang, Y.; Zhang, Y.; Yue, Y.; Zhang, J.; Qian, G. Controlling Role of CaClOH in the Process of Dechlorination for Municipal Solid Incineration Fly Ash Utilization. *ACS ES&T Eng.* **2022**, *2*, 2150–2158.
57. GB/T 18046-2017; China National Standardization Administration, Ground Granulated Blast Furnace Slag Used for Cement Mortar and Concrete. National Standards of the People's Republic of China: Beijing, China, 2017.
58. GB/T 1596-2017; China National Standardization Administration, Fly Ash Used for Cement and Concrete. National Standards of the People's Republic of China: Beijing, China, 2017.

59. Sun, Z.; Vollpracht, A. Isothermal calorimetry and in-situ XRD study of the NaOH activated fly ash, metakaolin and slag. *Cem. Concr. Res.* **2018**, *103*, 110–122. [[CrossRef](#)]
60. Zhang, Z.; Provis, J.L.; Zou, J.; Reid, A.; Wang, H. Toward an indexing approach to evaluate fly ashes for geopolymer manufacture. *Cem. Concr. Res.* **2016**, *85*, 163–173. [[CrossRef](#)]
61. GB/T 17671-2021; China National Standardization Administration, Test Method of Cement Mortar Strength (ISO Method). National Standards of the People's Republic of China: Beijing, China, 2021.
62. EN 196-1:2016; European Committee for Standardization, Methods of Testing Cement—Part 1: Determination of Strength. European Standards: Brussels, Belgium, 2015.
63. GB/T 15555.4-1995; China National Standardization Administration, Solid Waste—Determination of Chromium(VI)—1, 5-Diphenylcarbohydrazide Spectrophotometric Method. National Standards of the People's Republic of China: Beijing, China, 1995.
64. Xue, J.; Briseghella, B.; Huang, F.; Nuti, C.; Tabatabai, H.; Chen, B. Review of ultra-high performance concrete and its application in bridge engineering. *Constr. Build. Mater.* **2020**, *260*, 119844. [[CrossRef](#)]
65. Guo, X.; Hu, W.; Shi, H. Microstructure and self-solidification/stabilization (S/S) of heavy metals of nano-modified CFA-MSWIFA composite geopolymers. *Constr. Build. Mater.* **2014**, *56*, 81–86. [[CrossRef](#)]
66. GB 8978-1996; China National Standardization Administration, Integrated Wastewater Discharge Standard. National Standards of the People's Republic of China: Beijing, China, 1996.
67. GB 14848-2017; China National Standardization Administration, Standard for Groundwater Quality. National Standards of the People's Republic of China: Beijing, China, 2017.

Disclaimer/Publisher's Note: The statements, opinions and data contained in all publications are solely those of the individual author(s) and contributor(s) and not of MDPI and/or the editor(s). MDPI and/or the editor(s) disclaim responsibility for any injury to people or property resulting from any ideas, methods, instructions or products referred to in the content.